Clinical Biomechanics 71 (2020) 201–207

Contents lists available at ScienceDirect

Clinical Biomechanics

journal homepage: www.elsevier.com/locate/clinbiomech

The early failure of the gamma nail and the dynamic hip screw in femurs with a wide medullary canal. A biomechanical study of intertrochanteric fractures

Marcin Ceynowa[a,*], Krzysztof Zerdzicki[b], Pawel Klosowski[b], Rafał Pankowski[a], Marek Rocławski[a], Tomasz Mazurek[a]

[a] Department of Orthopedic Surgery, Medical University of Gdańsk, ul. Nowe Ogrody 1-6, 80-803 Gdańsk, Poland
[b] Faculty of Civil and Environmental Engineering, Gdansk University of Technology, Gabriela Narutowicza 11/12, 80-233 Gdańsk, Poland

ARTICLE INFO

Keywords:
Dynamic hip screw
Gamma nail
Intertrochanteric fracture
Biomechanical study

ABSTRACT

Background: Intertrochanteric fractures may occur in a bone with a wide medullary canal that may lead to significant mobility of a intramedullary nail, contrary to an extramedullary device. This study evaluates the Dynamic Hip Screw and the gamma nail in AO 31.A2.1 fractures in these circumstances.

Methods: Synthetic femora with canals drilled to 18 mm were used. Five fixation types were examined: a 2 - hole and a 4 – hole Dynamic Hip Screw with a 2 - hole plate, a standard gamma nail with dynamic and static distal locking and a long gamma nail.

The specimens were tested with cyclic axial loading, from 500 N increasing of 50 N increments in each cycle. Force at failure, overall stiffness, stiffness at the fracture site, location and mode of failure were recorded.

Findings: The short gamma nails dislocated into varus under preload because the nail migrated laterally. The Dynamic Hip Screw was initially stable, but some specimens rotated around the lag screw. The gamma nail was rotationally stable. Both implants failed through femur fracture. The long gamma nailed failed by screw cut – out at forces lower than the ultimate force of the short gamma nail.

Interpretation: This study shows that the gamma nail is unstable in a large medullary canal but offers better rotational stability of the proximal fragment. A modification of the nail design or the operative technique may be considered.

1. Introduction

The fixation of intertochanteric femoral fractures has been intensively studied in the past decades. Although biomechanical data suggests that the intramedullary fixation is superior to the extramedullary, modern clinical data show similar results in patients treated with different types of implants (Barton et al., 2010; Bhandari et al., 2009; Liu et al., 2010; Saarenpää et al., 2009). There are concerns about a higher prevalence of fractures of the femur in the gamma nail, but new designs and correct operative technique seem to have resolved this issue more recently (Bhandari et al., 2009; Bojan et al., 2010). On the other hand, the intramedullary devices perform better in grossly unstable fractures (Kokoroghiannis et al., 2012; Palm et al., 2016; Schipper et al., 2004).

Biomechanical studies, even with high quality clinical data available, are invaluable in assessing newly designed implants (Basso et al., 2014, 2012; Marmor et al., 2015; Queally et al., 2014), or in explaining the reasons for fixation failure observed in vivo and providing modifications in operative techniques that may lower the complication rate (Kaiser et al., 1997; Kukla et al., 2001; Kuzyk et al., 2012; Lenich et al., 2011).

Clinical and biomechanical studies compare implants with regard to revision rate, screw cut – out or fracture of the bone. Less attention is given to stability with malreduction or to secondary dislocation. Assessment of dislocation after fixation and its impact on patient's performance is very difficult to establish on standard radiographs (Barton et al., 2010; Bojan et al., 2010; Kim et al., 2001).

The aim of this study was to evaluate the stability DHS and the gamma nail fixation in AO 31.A2.1 fractures with a wide medullary canal. An intramedullary device inserted in a medullary canal wider than the diameter of the nail may provide significant mobility of the nail in the canal and therefore lead to early dislocation of the fixation,

* Corresponding author at: Department of Orthopedics and Traumatology, Medical University of Gdańsk, ul. Nowe Ogrody 1-6, 80-803 Gdańsk, Poland.
E-mail addresses: mceynowa@gumed.edu.pl (M. Ceynowa), krzysztof.zerdzicki@pg.edu.pl (K. Zerdzicki), klosow@pg.edu.pl (P. Klosowski).

https://doi.org/10.1016/j.clinbiomech.2019.11.006
Received 19 August 2019; Accepted 11 November 2019

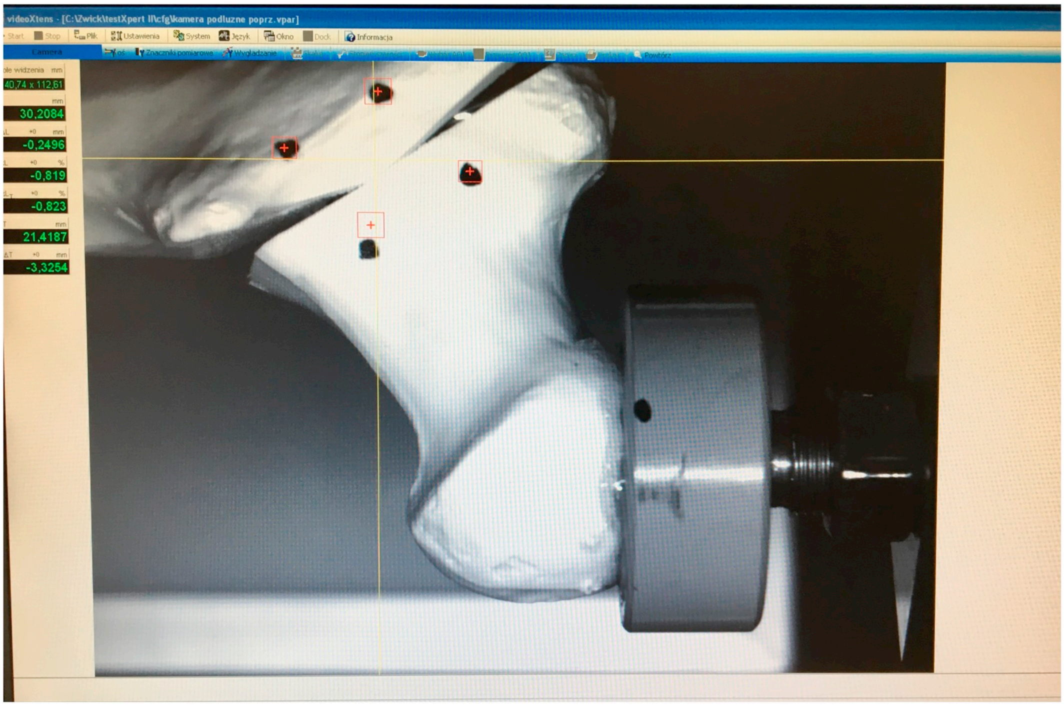

Fig. 1. A screenshot of an optical extensometer view with vertical and horizontal axis of data acquisition. Note that one of the horizontal acquisition windows lost track of its marker.

when compared to extramedullary device, which is securely fixed to the femoral cortex.

Moreover, the usefulness of an optical extensometer to evaluate mobility at the fracture site was assessed separately.

2. Methods

2.1. Sample preparation

Synthetic osteoporotic left femora (LD2350.01, cortical low density/soft cancellous bone, Synbone AG, Neugutstrasse 4, 7208 Malans, Switzerland) were used (Ozkan et al., 2015). The canals were drilled to 18 mm width up to the level of the lesser trochanter (Marmor et al., 2015; Rog et al., 2017; Sommers et al., 2007). The bones were assigned to five groups: a standard Dynamic Hip Screw with 2 - hole plate, a DHS with 4 holes, a standard gamma nail with dynamic and static distal locking and a long gamma nail. The femora were pre-drilled for fixation with the original instrument set. Then intertrochanteric fractures (AO 31.A2.1) were created with custom templates. The first cut was at 35^0 to the long axis of the femur, starting at the apex of the greater trochanter. The second cut that simulated comminution was performed at the distal fragment at 20^0 to the first cut, starting at the middle of the first cut, effectively removing the lesser trochanter region (Weiser et al., 2015). The samples were then fixed with original implants (Omega3 130^0, and Gamma3 125^0, Stryker GmBH, 2825 Airview Boulevard, Kalamazoo, MI 49002 USA). The correct position of the lag screw was ensured (Baumgaertner et al., 1995; Kuzyk et al., 2012). Its position was evaluated on AP and axial radiographs by calculating the distance between the intersection of the long axis of the neck with the femoral head cortex on both projections (Ceynowa et al., 2019) and the similar intersection of the long axis of the screw (Lenich et al., 2011).

2.2. Test protocol

The femora were fixed with the custom made clamps into the Zwick-Roell Z020 testing machine in 8^0 abduction in the coronal plane and vertically in the sagittal plane (Marmor et al., 2015), with the distal fixation in each specimen flush above the femoral condyles. The specimens were tested with the axial loading.

There is a range of testing protocols used in biomechanical studies of femoral fractures, utilizing both static (Haynes et al., 1997; Ozkan et al., 2015; Selvan et al., 2004) and cyclic loading (Aminian et al., 2007; Kwak et al., 2018). Cyclic loading more closely resembles the mechanics of the fixed fracture in a walking patient. The number of cycles varies, but the commonly used 10,000 cycles protocol attempts to simulate walking of a patient over a 6 week period until healing occurs (Aminian et al., 2007; Kwak et al., 2018; Weiser et al., 2015). This assumption, theoretically sound, is biased because the transfer of loads changes from occurring primary through the implant to be transferred through the bone as healing progresses over this period (Schneider et al., 2001). The loading during cycles is also variable, but the upper load of 1400 N is considered to be the equivalent of the weight of 70 kg person (Aminian et al., 2007). In many instances, the 10,000 cycles and 1400 N protocol is modified according to the needs of the study (Aminian et al., 2007; Kwak et al., 2018; Weiser et al., 2015). Taking into consideration all the limitations in study protocol, the progressive cyclic loading was chosen as a previously tested, reliable, and less time consuming than other protocols (Kaiser et al., 1997; Kukla et al., 2001).

The test protocol included the preload of 100 N and ten conditioning cycles from 100 N to 500 N (Marmor et al., 2015), with the displacement rate of 10 mm/min. The test phase consisted of the cyclic loading between 100 N and the maximum force that increased at a rate of 50 N at each cycle (Kaiser et al., 1997; Kukla et al., 2001) until failure or until force of 1400 N (Aminian et al., 2007). The force at failure was defined by the drop of the applied force (Haynes et al., 1997) or inability to increase force value with increasing standard travel (Kaiser et al., 1997; Selvan et al., 2004).

The load and displacement data were taken from the force gauge of the testing machine and from displacement of its traverse (standard travel). The stiffness of the construct was calculated from the load/standard travel curve from the last three conditioning cycles (Rog et al., 2017). An optical extensometer was used to directly measure the displacement at the fracture site (Fig. 1). Unfortunately, with

Table 1
Results of the testing protocol.

Fixation	Force at failure (N)	Stiffness standard (N/mm)	Stiffness extensometer (N/mm)
DHS 2 – hole (n = 11)	452.73 SD = 131 R: 251–574	177.03 (n = 3) R: 137.74–208.62	3818.3 (n = 3) R: 1546.39–6250
DHS 4 – hole (n = 10)	578.1 SD = 99.16 R: 421–679	229.3 (n = 7) SD = 44.22 R: 143.27–268.8	7256.65 (n = 7) SD = 6808.29 R: 1351.35–21,428.6
Gamma dynamic locking (n = 9)	823.77 SD = 135.45 R: 656–1070	322.25 SD = 80.83 R: 234.01–436	34,807.92 SD = 44,381.02 R: 7894.74–150,000
Gamma static locking (n = 9)	830 SD = 156.31 R: 631–1030	312.34 SD = 80.52 R: 200–453.2	19,053.72 SD = 23,269.14 R: 4838.71–75,000
Gamma long (n = 7)	1400 SD = 0	770.88 SD = 53.83 R: 681.82–838	43,452.38 SD = 24,039.07 R: 16,666.67–75,000

dislocations > 2 mm the extensometer lost track of the markers and only data from conditioning cycles could be considered reliable. Data from the last three cycles was used to calculate stiffness at the fracture site.

After testing, the specimens were examined for the location of the fractures, distal screw migration or bending of the implant. The femoral heads of all specimens was cut in line with the lag screw to see whether any cut – out occurred.

The statistical evaluation was performed using Statistica 13.3 software. The Shapiro – Wilk test was used to assess normal distribution. The t-Student test was used for parametric, and the U Mann Whitney test for non-parametric evaluation.

3. Results and discussion

The results are provided in Table 1.

3.1. Force to fracture

The force to fracture assessed in biomechanical studies is most likely of little relevance, because the significant differences seen in vitro are not seen in patients. Therefore the obvious differences in force to fracture in different implants in this study should be probably disregarded. With modern designs and improvement in operative technique, both the DHS and the gamma nail should be considered reliable in treatment of those fractures, and most of the complications related to the earlier designs of the gamma nail have been overcome (Bhandari et al., 2009; Schipper et al., 2004).

The results show that the 2 – hole DHS has the lowest force to fracture. The 4 – hole DHS is approximately 20% stronger than the 2 – hole DHS ($p < 0.05$). This result stands in contrast to previous biomechanical studies that showed similar forces to fracture in both implant types (Rog et al., 2017).

There are no differences in the force to failure between both types of short gamma nail distal locking. The short gamma nail is nearly twice as strong as the 2 – hole DHS and approximately 30% stronger than the 4 – hole DHS.

The long gamma nail withstood without a fracture forces 40% greater than the short gamma nails, almost two times the forces of fracture of the 4 – hole DHS and nearly three times as much as the 2 – hole DHS. However, it failed through screw cut-out, what will be described in detail in Section 3.3.

All the differences in this section were statistically significant ($p < 0.05$).

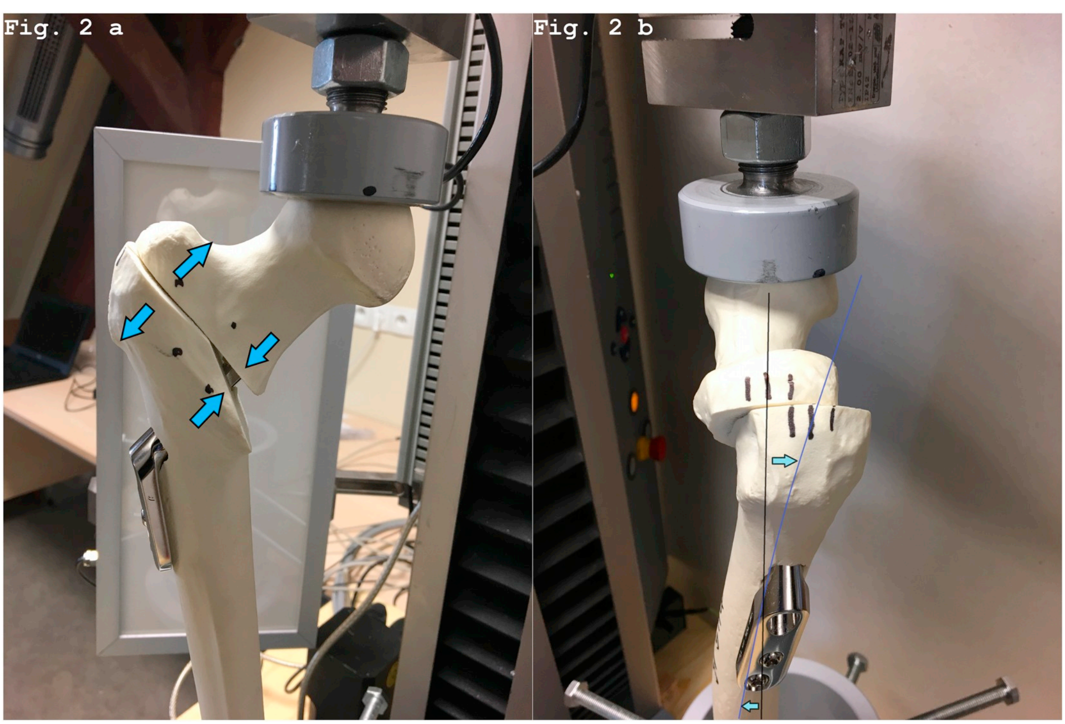

Fig. 2. Rotational failure of the DHS.
a. Under axial loading, the upper part of fracture is decompressed and the friction therefore lowered. The lower part is unsupported and does not provide friction in unstable fractures.
b. The femur bends under load in line with physiological bending of the bone, while the proximal fragment does not move, producing rotation in line with the lag screw.

3.2. Early dislocation of the short gamma nail and the DHS

Some biomechanical studies attempt to quantify failure as displacement of the fracture (Aminian et al., 2007; Barton et al., 2010; Bojan et al., 2010; Kaiser et al., 1997). Most clinical studies do not take into account fracture stability, but only complication rate (Kokoroghiannis et al., 2012). In unstable comminuted fractures, the sliding hip screw had a higher reoperation rate compared to the intramedullary nail, and fracture reduction is an independent risk factor for the operation (Palm et al., 2016; Schipper et al., 2004).

3.2.1. Rotation failure of the DHS

The DHS is prone to significant rotation at the fracture site, that can be assessed quantitatively only to a limited extent. In this study, the critical rotation has been set as 5 mm of the rotational displacement at the level of greater trochanter (Aminian et al., 2007). 6/11 2-hole specimens and 4/10 4-hole specimens demonstrated extensive rotation of the proximal fragment at the fracture site (Fig. 2a,b).

The comparison of the lag screw's position in the femoral head showed that the rotated specimens were on average in the same position on the AP view (rotated specimens: 2.8 mm, *SD* = 3.08, *R*: 0–7; not rotated:: 2.3 mm, *SD* = 2.05, *R*: 0–6; gamma nails: 2.05 mm, *SD* = 2.22, *R*: 2–3), but in the axial view the rotated DHS the screw had a slightly more eccentric position than the not rotated DHS and the gamma nail (rotated specimens: 3 mm, *SD* = 2.04, *R*: 0–7; not rotated:: 1.5 mm, *SD* = 1.8, *R*: 0–5; gamma nail: 2.3 mm, *SD* = 1.8, *R*: 0–3). Moreover, in the rotated group the screw tended to be placed posterior to the axis, and in the not rotated, anterior to the axis (Lenich et al., 2011). Those differences were statistically not significant.

The rotation at the fracture side was considered to be the result of increased anterior bowing of the distal fragment under axial compression, in line with the physiological bowing of the bone (Fig. 2b). The proximal fragment did not rotate in the clamp. After testing none of them showed any signs of lag screw migration.

In fracture fixation with a lag screw, the rotation is prevented by friction of the compressed bone fragments. In intertrochanteric fractures, when axial force is applied, the fracture is forced into varus, where the bone fragments above the line of the screw are decompressed and friction diminishes. In stable fractures where the bone provides medial support, the fragments below the screw are compressed what prevents rotation (Fig. 2a). Without medial support, the rotation is prevented mostly by friction of the lag screw against its canal (Kwak et al., 2018). Not all DHS fixations rotated probably because of some minor differences in the lag screw placement or fracture preparation made some specimens more resistant to this complication (Lenich et al., 2011). The analysis of the lag screw position failed to provide any definitive reasons for this complication.

None of the gamma nails showed any rotation of the fragments. Since both types of screws (DHS and gamma) fail in similar torque magnitudes (Lenich et al., 2011), the resistance to rotation should be attributed to the fact that the proximal end of the nail is located in a groove in the proximal fragment of the femur, what stabilizes the proximal fragment in rotation (Fig. 3). The effect of the screw construct, however, cannot be definitely ruled out in this study (Kwak et al., 2018).

3.2.2. Movement of the gamma nail in the medullary canal

Both the dynamic and the static locking short gamma nails dislocated into varus under gravity or during the preload in the testing machine (Fig. 4a,b). This initial failure could not be recorded by the testing machine, since they occurred in the pre-loading phase. This dislocation was due to the large discrepancy in the diameters of the medullary canal (18 mm) and the distal part of the nail (11 mm), and the tip of the nail migrated laterally as far as the lateral cortex (Fig. 4a,b). To the best of our knowledge, his phenomenon has not been previously reported (Bhandari et al., 2009; Marmor et al., 2015; Queally et al., 2014). Only few biomechanical studies used reaming to 18 mm canal width (Marmor et al., 2015; Rog et al., 2017; Sommers et al., 2007), and even fewer evaluate an intramedullary device, where this problem can be encountered (Marmor et al., 2015).

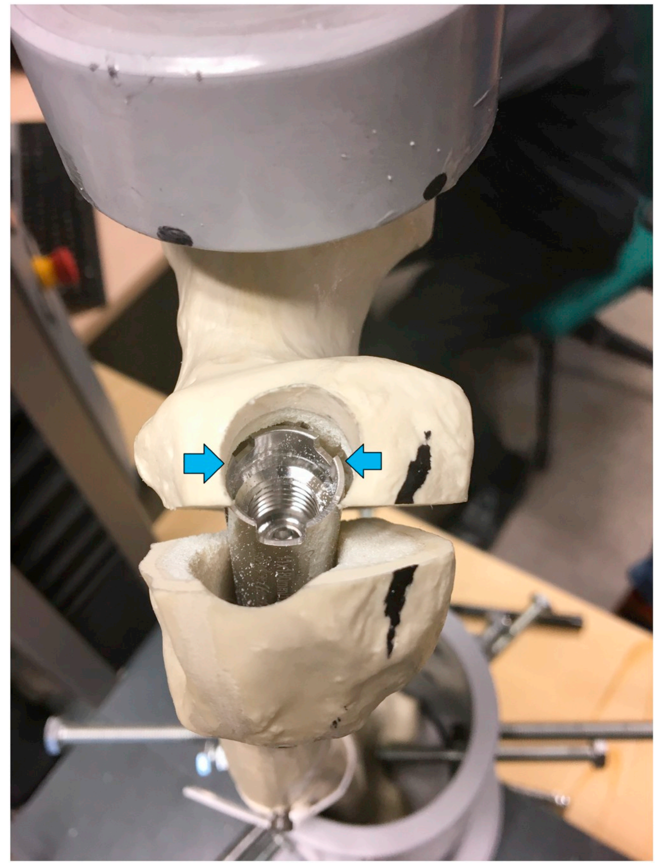

Fig. 3. The gamma nail under axial loading. The arrows show the groove in the bone that protects from rotation of the proximal fragment.

Afterwards the nails provided good stability of the fragments. During testing, all the nails failed by fracture, with no differences in occurrence of this failure mode between dynamic and static locking constructs.

The initial medial migration of the tip of the gamma nail may be of utmost importance regarding the fracture of the femur (Bhandari et al., 2009; Liu et al., 2010; Parker and Handoll, 2008; Queally et al., 2014). The increased stress at its tip may be a contributing factor to fractures (Rosenblum et al., 1992). Although the tip stabilized in its lateral position, the micromotion at the tip may lead to progressive destruction of the bone and ultimately to fracture (Rosenblum et al., 1992). Moreover it should be noted that the lateral dislocation of the tip and the resulting compression of the lateral cortex by the nail may always occur, but it may not be readily visible in narrower canals.

None of the long gamma nails showed similar mobility in the medullary canal despite their same diameters as the short nails because it was locked distally in both holes. The distal hole is oblong, like the single locking hole in the short nails, and the proximal hole is oval and tight around the screw (Fig. 5) what prevents mobility of the nail end when axial force is applied. When only the screw from the oval hole was removed, the nail end could easily move in the medullary canal. Moreover, when an additional screw was inserted in the oblong hole of the short nail to tighten the hole, the nail end retained its position in the medullary canal.

The varus dislocation can also be prevented by a simple modification of the operative technique. In a reduced fracture, after the nail is inserted, the tip can be placed against the lateral cortex by abducting

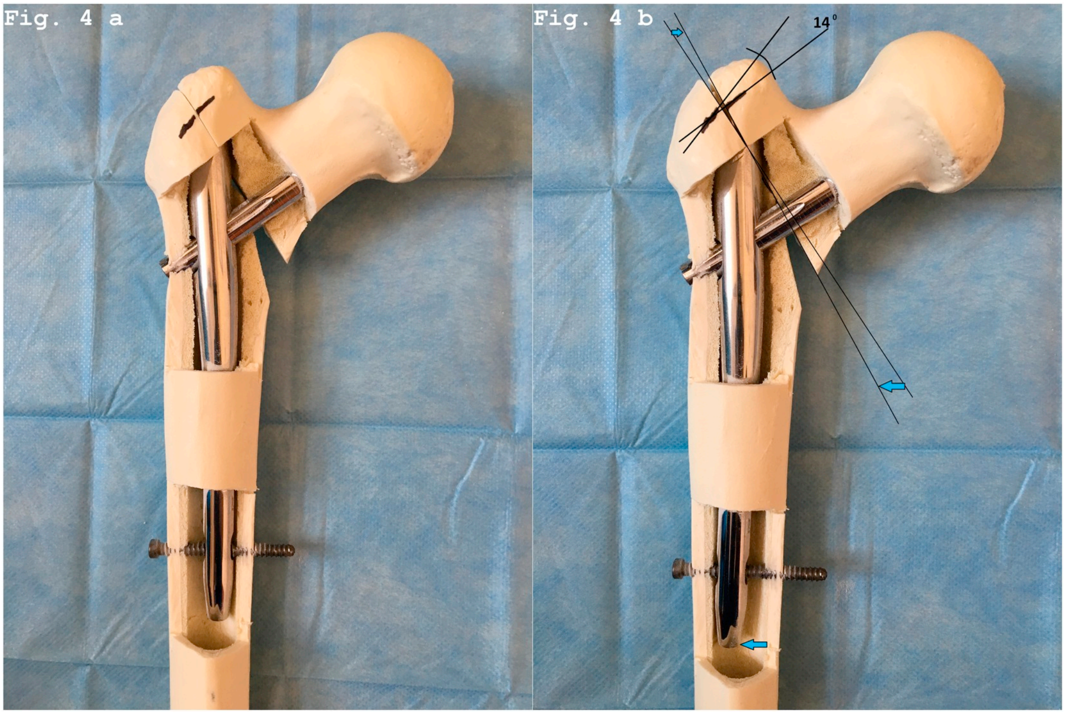

Fig. 4. The varus dislocation of the short gamma nail.
a. The fracture is fixed and reduced properly, the windows in the bone show medial position of the nail tip.
b. With minimal axial force applied, the fracture dislocates into varus while the nail tip moves from its medial to lateral position in the medullary canal.

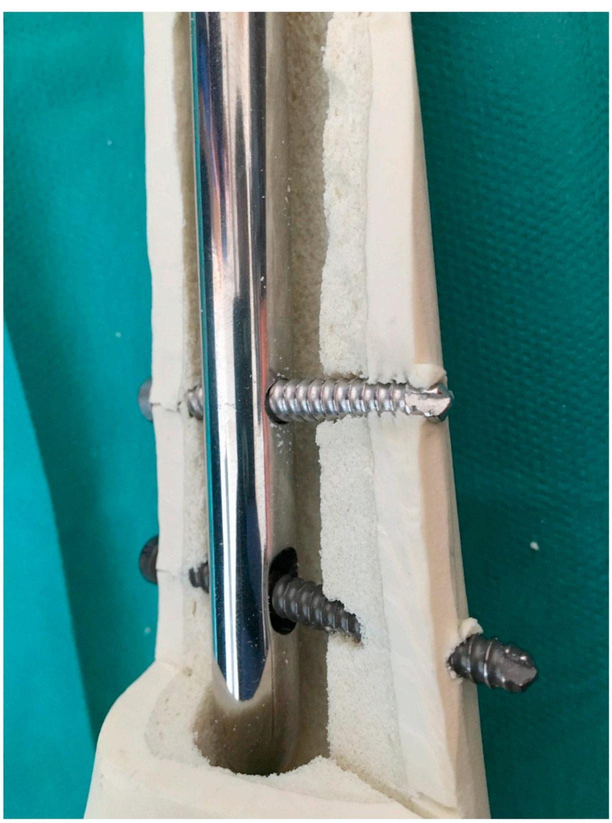

Fig. 5. Distal locking of the long gamma nail. The upper hole is round and tight around the screw, what protects the nail tip from moving from medial to lateral. The lower hole is oblong and unstable.

the distal part of the targeting device and forcing the nail into varus in the medullary canal before placing the guide wire for the lag screw. After completing the fixation, the nail end remains its position against the lateral cortex. However, this modification will prevent only varus dislocation, but the problem of stress rise at the tip of the nail persists.

Alternatively, a modification of the nail construct or use of a nail with an oval hole would most likely prevent its mobility. Moreover, maintaining nail tip position centrally in the canal may change force distribution in the bone – nail construct and help avoid stress riser formation at the nail end. Proving this, however, will require further biomechanical studies.

3.3. The cut-out of the lag screw

All the long gamma nails survived the cyclic testing phase up to 1400 N load. No signs of distal screw migration, fracture of the femur, or bending of the nail were found. The load/displacement curve, after a period of symmetric cycles with sharp peaks, showed a period of elongated cycles. This part of the curve was accompanied with visible varus dislocation at the fracture site. After testing when the femoral heads were cut, they showed lag screw migration in the head. Most likely, the migration began with the first elongated peak, and ended with the last elongated peak, where the lag screw stabilized again flush to the subchondral part of the specimen as in pending screw cut – out (Baumgaertner et al., 1995; Bojan et al., 2010; Haynes et al., 1997; Lenich et al., 2011; Palm et al., 2016). It has been considered that the beginning of the cut-out on the load – displacement curve is more important than ultimate migration (Aminian et al., 2007), because once the screw begins to migrate, it becomes loose and further migration progresses (Lenich et al., 2011). No such widening was observed in any of the DHS and short gamma nail fixations in this study (Fig. 6).

The gamma long force at cut-out beginning was $F = 726{,}14$ N ($SD = 107{,}33$, R: 600–870). The force at cut – out end $F = 1037.29$ ($SD = 135.1$, R: 890–1247). The force at cut-out begin was significantly greater than the force at failure when compared to 2 – hole DHS

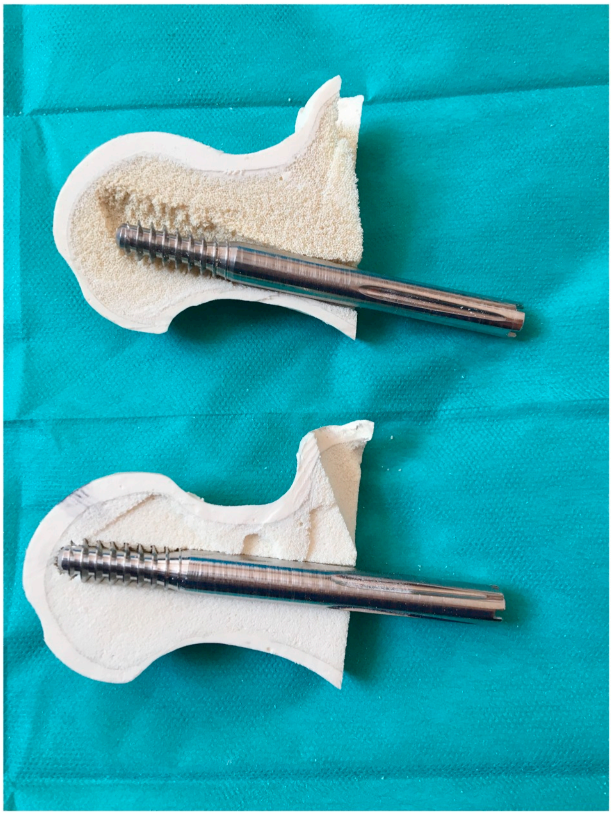

Fig. 6. Femoral heads cut in line with the lag screw. The upper specimen from a long gamma nail shows extensive loosening and pending cut – out, the lower specimen from a short gamma nail has no signs of loosening.

fixations (approximately 37%) and 4 – hole DHS (approximately 20%), but smaller when compared to dynamic and static short gamma nail (approximately 12%). The force at cut – out end was greater than the force at failure to the gamma nail (approximately 20%). All the differences were statistically significant ($p < 0.05$).

The differences in mode of failure can be attributed to different stiffness of the fixation types. The overall stiffness increases with the length of the distal part of the fixation (2 – hole plate v/s 4 – hole plate v/s short gamma nail v/s long gamma nail). The long gamma nail is stiffer than other fixation types. The deformation of the whole bone is lower than with other constructs, and with shorter constructs the distal part of the bone can bend under axial load. While the bone bends, the stresses cumulate at the end of the shorter implants, but in stiffer long gamma nail the fixation of the lag screw in the femoral head is the point of least resistance.

Varus collapse can also be attributed to screw type, as has been proven for different intramedullary nails (Kwak et al., 2018), since the DHS and the gamma nail have different screws. However, the short and the long gamma nail have the same type of screws, and the cut-out was seen only in the long gamma nail. The DHS and the short gamma nails did not show this complication, therefore in this study it is unlikely that the screw construct was the reason for the differences in its occurrence.

3.4. The usefulness of an extensometer

The stiffness from the standard travel is a measure of both the dislocation at the fracture site and the bending of the bone before fracture (Kuzyk et al., 2012). The stiffness calculated from the extensometer is much greater than the stiffness of the whole fixed fracture model. The results were extremely variable and the differences were statistically not significant.

The used extensometer's software provides interesting additional information to the standard biomechanical measurements. It can show very small dislocations along a single axis (Fig. 1) very close to the fracture line. This is suboptimal for multiplanar or rotational dislocations. The acquired stiffness results are influenced by changes even of 0.01 mm. Despite all the limitations of the method, it shows that the stiffness at the fracture site is invariably much greater than the stiffness measured from the clamps of the testing machine. The type and length of the implant, as well as the remaining length of the tested bone may influence traditionally acquired results significantly, but not necessarily directly influence the stability of the fracture itself. This methodology requires further software refinement to provide more reliable results.

4. Conclusions

The most important finding of this study is that the intramedullary devices are prone to early dislocation in patients with a large medullary canal fixed with a nail relatively smaller in diameter and a locking hole that is loose around the screw. This can be overcome by the modification of the operative technique, small improvements in the nail design, or the use of a long gamma nail with distal locking in the oval hole. However, the long gamma nail may be more prone to screw cut – out than the short nail, therefore the risks and benefits of long versus short gamma nail should be carefully assessed in future clinical studies.

The DHS provides better initial stability than the short gamma nail, but is prone to rotation on the fracture site, what is not observed with the gamma nail. In contrast to other biomechanical studies (Rog et al., 2017) the 4 – hole DHS proved stronger than the 2 – hole DHS.

The use of an extensometer to evaluate fracture site mobility may provide additional valuable information inaccessible clinically, but the method requires further refinement.

The results of this study require further investigation in clinical studies. Most importantly, the possibility of the lateral dislocation of the nail tip in large medullary canals and its potential influence on treatment should be verified. Moreover, the rotational displacement of the DHS found in this study calls for a more detailed assessment of secondary dislocation on follow-up radiographs when evaluating outcome of intertrochanteric fracture treatment.

Funding

This work was supported by the National Science Centre, Poland [NCN 2018/02/X/NZ5/02070].

Declaration of competing interest

None.

Appendix A. Supplementary data

Supplementary data to this article can be found online at https://doi.org/10.1016/j.clinbiomech.2019.11.006.

References

Aminian, A., Gao, F., Fedoriw, W.W., Zhang, L.Q., Kalainov, D.M., Merk, B.R., 2007. Vertically oriented femoral neck fractures: mechanical analysis of four fixation techniques. J. Orthop. Trauma 21, 544–548. https://doi.org/10.1097/BOT.0b013e31814b822e.

Barton, T.M., Gleeson, R., Topliss, C., Greenwood, R., Harries, W.J., Chesser, T.J.S., 2010. A comparison of the long gamma nail with the sliding hip screw for the treatment of AO/OTA 31-A2 fractures of the proximal part of the femur: a prospective randomized trial. J. Bone Joint Surg. Am. 92, 792–798. https://doi.org/10.2106/JBJS.I.00508.

Basso, T., Klaksvik, J., Syversen, U., Foss, O.A., 2012. Biomechanical femoral neck fracture experiments - a narrative review. Injury 43, 1633–1639. https://doi.org/10.1016/j.injury.2012.03.032.

Basso, T., Klaksvik, J., Syversen, U., Foss, O. a, 2014. A biomechanical comparison of composite femurs and cadaver femurs used in experiments on operated hip fractures. J. Biomech. 47, 3898–3902. https://doi.org/10.1016/j.jbiomech.2014.10.025.

Baumgaertner, M.R., Curtin, S.L., Lindskog, D.M., Keggi, J.M., 1995. The value of the tip-

apex distance in predicting failure of fixation of peritrochanteric fractures of the hip. JBJS 77.
Bhandari, M., Schemitsch, E., Jönsson, A., Zlowodzki, M., Haidukewych, G.J., 2009. Gamma nails revisited: gamma nails versus compression hip screws in the management of intertrochanteric fractures of the hip: a meta-analysis. J. Orthop. Trauma 23, 460–464. https://doi.org/10.1097/BOT.0b013e318162f67f.
Bojan, A.J., Beimel, C., Speitling, A., Taglang, G., Ekholm, C., Jönsson, A., 2010. 3066 consecutive gamma nails. 12 years experience at a single centre. BMC Musculoskelet. Disord. 11. https://doi.org/10.1186/1471-2474-11-133.
Ceynowa, M., Rocławski, M., Pankowski, R., Mazurek, T., 2019. The position and morphometry of the fovea capitis femoris in computed tomography of the hip. Surg. Radiol. Anat. 41, 101–107. https://doi.org/10.1007/s00276-018-2097-y.
Haynes, R.C., Pöll, R.G., Miles, A.W., Weston, R.B., 1997. Failure of femoral head fixation: a cadaveric analysis of lag screw cut-out with the gamma locking nail and AO dynamic hip screw. Injury 28, 337–341. https://doi.org/10.1016/S0020-1383(97)00035-1.
Kaiser, W., Burmester, J., Hausmann, H., Guliemos, V., Haetzel, M., Merker, H., 1997. Vergleichende Stabilitätsprüfungen von DHS- und g -Nagel-Osteosynthesen bei instabilen pertrochantären Femurosteotomien. Langenbecks Arch. Chir. 382, 100–106.
Kim, W.Y., Han, C.H., Park, J.I., Kim, J.Y., 2001. Failure of intertrochanteric fracture fixation with a dynamic hip screw in relation to pre-operative fracture stability and osteoporosis. Int. Orthop. 25, 360–362. https://doi.org/10.1007/s002640100287.
Kokoroghiannis, C., Aktselis, I., Deligeorgis, A., Fragkomichalos, E., Papadimas, D., Pappadas, I., 2012. Evolving concepts of stability and intramedullary fixation of intertrochanteric fractures - a review. Injury 43, 686–693. https://doi.org/10.1016/j.injury.2011.05.031.
Kukla, C., Pichl, W., Prokesch, R., Jacyniak, W., Heinze, G., Gatterer, R., Heinz, T., 2001. Femoral neck fracture after removal of the standard gamma interlocking nail: a cadaveric study to determine factors influencing the biomechanical properties of the proximal femur. J. Biomech. 34, 1519–1526. https://doi.org/10.1016/S0021-9290(01)00157-9.
Kuzyk, P.R.T., Zdero, R., Shah, S., Olsen, M., Waddell, J.P., Schemitsch, E.H., 2012. Femoral head lag screw position for cephalomedullary nails: a biomechanical analysis. J. Orthop. Trauma 26.
Kwak, D.K., Kim, W.H., Lee, S.J., Rhyu, S.H., Jang, C.Y., Yoo, J.H., 2018. Biomechanical comparison of three different intramedullary nails for fixation of unstable basicervical intertrochanteric fractures of the proximal femur: experimental studies. Biomed. Res. Int. 2018. https://doi.org/10.1155/2018/7618079.
Lenich, A., Bachmeier, S., Prantl, L., Nerlich, M., Hammer, J., Mayr, E., Al-Munajjed, A.A., Füchtmeier, B., 2011. Is the rotation of the femural head a potential initiation for cutting out? A theoretical and experimental approach. BMC Musculoskelet. Disord. 12. https://doi.org/10.1186/1471-2474-12-79.
Liu, M., Yang, Z., Pei, F., Huang, F., Chen, S., Xiang, Z., 2010. A meta-analysis of the Gamma nail and dynamic hip screw in treating peritrochanteric fractures. Int. Orthop. 34, 323–328. https://doi.org/10.1007/s00264-009-0783-4.
Marmor, M., Elliott, I.S., Marshall, S.T., Yacoubian, Shahan V., Yacoubian, Stephan V., Herfat, S.T., 2015. Biomechanical comparison of long, short, and extended-short nail construct for femoral intertrochanteric fractures. Injury 46, 963–969. https://doi.org/10.1016/j.injury.2015.03.005.
Ozkan, K., Turkmen, I., Sahin, A., Yildiz, Y., Erturk, S., Soylemez, S., 2015. A biomechanical comparison of proximal femoral nails and locking proximal anatomic femoral plates in femoral fracture fixation. A study on synthetic bones. Indian J. Orthop. 39, 347–351. https://doi.org/10.4103/0019-5413.156220.
Palm, H., Jacobsen, S., Sonne-Holm, S., Gebuhr, P., 2016. Integrity of the lateral femoral wall in intertrochanteric hip fractures. J. Bone Joint Surg. Am. 89, 470–475. https://doi.org/10.2106/00004623-200703000-00002.
Parker, M.J., Handoll, H.H.G., 2008. Gamma and other cephalocondylic intramedullary nails versus extramedullary implants for extracapsular hip fractures in adults. Cochrane Database Syst. Rev. https://doi.org/10.1002/14651858.CD000093.pub4.
Queally, J.M., Harris, E., Handoll, H.H., Parker, M.J., 2014. Intramedullary nails for extracapsular hip fractures in adults. Cochrane Database Syst. Rev. 9, Cd004961. https://doi.org/10.1002/14651858.CD004961.pub4.
Rog, D., Grigsby, P., Hill, Z., Pinette, W., Inceoglu, S., Zuckerman, L., 2017. A biomechanical comparison of the two-and four-hole side-plate dynamic hip screw in an osteoporotic composite femur model. J. Orthop. Surg. 25. https://doi.org/10.1177/2309499017717199.
Rosenblum, S.F., Zuckerman, J.D., Kummer, F.J., Tam, B.S., 1992. A biomechanical evaluation of the gamma nail. J. Bone Joint Surg. (Br.) 74-B, 352–357.
Saarenpää, I., Heikkinen, T., Ristiniemi, J., Hyvönen, P., Leppilahti, J., Jalovaara, P., 2009. Functional comparison of the dynamic hip screw and the Gamma locking nail in trochanteric hip fractures: a matched-pair study of 268 patients. Int. Orthop. 33, 255–260. https://doi.org/10.1007/s00264-007-0458-y.
Schipper, I.B., Marti, R.K., Van Der Werken, C., 2004. Unstable trochanteric femoral fractures: Extramedullary or intramedullary fixation: review of literature. Injury 35, 142–151. https://doi.org/10.1016/S0020-1383(03)00287-0.
Schneider, E., Michel, M.C., Genge, M., Zuber, K., Ganz, R., Perren, S.M., 2001. Loads acting in an intramedullary nail during fracture healing in the human femur. J. Biomech. 34, 849–857. https://doi.org/10.1016/S0021-9290(01)00037-9.
Selvan, V.T., Oakley, M.J., Rangan, A., Al-Lami, M.K., 2004. Optimum configuration of cannulated hip screws for the fixation of intracapsular hip fractures: a biomechanical study. Injury 35, 136–141. https://doi.org/10.1016/S0020-1383(03)00059-7.
Sommers, M.B., Fitzpatrick, D.C., Madey, S.M., Vande Zanderschulp, C., Bottlang, M., 2007. A surrogate long-bone model with osteoporotic material properties for biomechanical testing of fracture implants. J. Biomech. 40, 3297–3304. https://doi.org/10.1016/j.jbiomech.2007.04.024.
Weiser, L., Ruppel, A.A., Nüchtern, J.V., Sellenschloh, K., Zeichen, J., Püschel, K., Morlock, M.M., Lehmann, W., 2015. Extra- vs. intramedullary treatment of pertrochanteric fractures: a biomechanical in vitro study comparing dynamic hip screw and intramedullary nail. Arch. Orthop. Trauma Surg. 135, 1101–1106. https://doi.org/10.1007/s00402-015-2252-4.